ASIAN JOURNAL OF CIVIL ENGINEERING (BUILDING AND HOUSING) VOL. 12, NO. 3 (2011)
PAGES 375-393

SEISMIC PERFORMANCE OF A VARIABLE STIFFNESS SYSTEM

M.R. Tabeshpour[*a], A.A. Golafshani[b] and M. Monzavi[b]
[a]Faculty of Engineering, Sabzevar Tarbiat Moallem University, Sabzevar, Iran
[b]Department of Civil Engineering, Sharif University of Technology, Tehran, Iran

ABSTRACT

In this paper a new ribbed bracing system (RBS) is proposed capable of performing as a variable stiffness system that can be used for controlling structural deformations and frequency shifting to compensate seismic energy. RBS has two important advantages. Because of ribbed system, the compressive member is rigidly moved like a piston and a cylinder and therefore it is a buckling prevented system. Also it is possible to use this system as a semi-active system by considering the story drifts and global structural damage and control the system if it is necessary to be open or closed based on the operational criteria assigned in the system. RBS has no need to any actuator and large power supply, but just a battery-size power supply to switch the ribbed mechanism to be on or off. RBS is composed of a ribbed supplemental part and a normal wind-bracing on each floor. Considering an appropriate criterion based on the storey drift, minimum number of bracing systems will be active on the height of structure during earthquake. In contrast with completely closed RBS (CC-RBS) by on-off bracing system arranged along the height of the building cause period shifting of the structure to the larger value. Three stages are considered in the numerical studies: conventional bracing frame (CBF), CC-RBS and semi-active RBS (SA-RBS). Damage indices and Fourier transforms are calculated in order to discuss on the efficiency of the proposed system. Nonlinear dynamic analysis of system has been carried out and structural behaviour has been investigated. Numerical results show the efficiency of CC-RBS in reducing structural damage and improving seismic energy. Also base shear is reduced when SA-RBS is used and structural damage is more uniform in this case.

Keywords: Ribbed bracing system (RBS); completely closed RBS (CC-RBS); semi-active RBS (SA-RBS); shifting frequency; fourier amplitude; damage index

1. INTRODUCTION

Nowadays seismic Retrofitting of existing buildings using innovative systems is becoming an important problem in earthquake engineering. Generally in the conventional bracing systems it is assumed that the braces buckle under a little compressive force and therefore

[*] E-mail address of the corresponding author: tabesh_mreza@yahoo.com (M.R. Tabeshpour)

input energy is dissipated by both nonlinear buckling and tension of the braces. Inelastic behaviour of the structures is only energy dissipating source in the conventional building codes. For example yielding of braces in tension and nonlinear buckling of these elements are considered as dissipating energy sources under seismic excitation. Nowadays using of the controllable systems for improving the structural behaviour with energy dissipation or altering the structural properties received a great deal of attention from earthquake researchers and engineers [1,2]. Semi-active control systems have a great importance among control systems, because of offering the reliability of passive control device and having the potential to achieve, or even surpass, the performance of fully active systems without requiring large power supply [3]. These systems have no actuator for imposing control force to structure and control the response of the structure with altering the physical properties of structural systems. In contrast to active control systems, semi-active control devices do not have the potential to destabilize the structural system.

Initial research on active control systems has focused on the response of force-type systems. For Examples active mass driver (AMD), uses the inertia of an auxiliary mass as the control force, and the Active Tendon System, applies a direct control force by operating an actuator [4,5]. These systems are relatively simple and easy to operate. However, as the structural system becomes more complex and the seismic motion stronger, considerable more energy is required to operate force-type systems. To overcome the energy problem, several hybrid and semi-active systems have been proposed. Examples include the hybrid mass damper (HMD), which is a combination of a passive tuned mass damper (TMD) and an active control actuator [6-8], the semi-active controllable fluid dampers based on electrorheological or magnetorheologocal fluids [9-10], friction control devices which are used either as energy dissipators within the lateral bracing of a structure or as component within sliding isolation systems [11], semi-active viscous fluid dampers [12] and stiffness control devices, which are used to modify the stiffness and thus the dynamic characteristics of the structure to which they are attached. The latter systems have been investigated by several researchers [13-15].

A semi-active variable stiffness system (AVS) for seismic response control of structure has been presented by Kobori et al. [16]. This system can actively change the structural stiffness based on producing a non-stationary and non-resonant condition in buildings during earthquakes. A schematic of the non-resonant control system (AVS) that installed to a chevron bracing is shown in Figure 1. Based on the characteristics of the excitation this system causes to alter the stiffness of the structure depending on locking or unlocking variable stiffness device (VSD). The main advantage of such systems is that the aforementioned energy problem is now satisfactorily addressed, since the VSD can be activated by a small amount of energy. The AVS system is very sensitive to time delay, which cannot be neglected in engineering application. Hence, the controlled structure has the likelihood of resonating when subjected to earthquakes. As the damping acts well to minimize the peak responses of the structures particularly in resonant condition so supplemental damping is considered to be appended on the AVS system and a new semi-active variable stiffness and damping (AVSD) system is proposed.

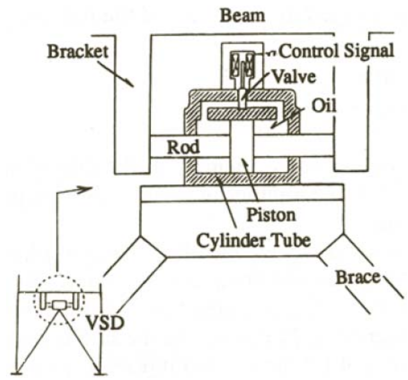

Figure 1. Outline of VSD mechanism [16].

Golafshani and Mirdamadi [17] proposed modified-Taylor device, which is accomplished by adding a number of bypass oil intakes to the Taylor device that can be switched on and off through the uses of control signals. In the proposed mechanism there are some closed containers into which the oil can flow. There are a number of orifices in the head of pistons that make the direct passive-type channels for the oil flow, similar to its passive type counterpart. So there is always some passive energy dissipating by oil, flowing due to the movement of piston relative to the container, when some drifts occur between adjacent floors. These valves are powered by battery size power supplies controlled by signals from the central control.

Golafshani et al. [18] proposed a new innovative high performance bracing system that consists of a simple mechanism based on semi-active control that can be installed in the braces as a supplemental part, Figure 2. In comparison with conventional brace system (CBS), ribbed bracing system (RBS) can absorbed seismic energy without causing large permanent drift in structure. In this system the buckling of compressive member is prevented and bracing can endure tension force in compressive region. Therefore by using of this system permanent stiffness is provided and structural response decreased. Also seismic damage in the equipped structure is concentrated in bracing system and dissipated hysteretic energy in other structural system decrease. Because this mechanism needs just a battery-size power supply, it can be accounted as an efficient semi-active control device.

The RBS device which is assembled in a desired location of the brace member, Figure 3, is made of high strength steel and consists of the following parts:

- Ribbed shaft
- Ribbed cylinder
- Switch + release plate
- Shell

There are springs in the inside rim of the shell that allow the ribbed shaft to squeeze outside toward the shell. When the ribbed shaft is under compressive axial force, ribs of shaft squeeze the cylinders ribs and push the cylinder outside toward the shell and the shaft moves freely inside. On the contrary, under tensile axial force the ribs of shaft and cylinder interact with each other and the shaft is locked so the system can tolerate tensile force, therefore a member that only endures tensile forces is developed. By developing this system, because of locking the ribs of the cylinder and shaft in each other, the nonlinear permanent deformation of the brace is compensated and the drift of the storey does not increase very much.

In addition to buckling preventing performance of the RBS (CC-RBS), it is possible to assign a simple control program to the system to have a more desired seismic behaviour. To achieve this goal an operational criterion is considered such as story drift, story damage index or global damage index. By this kind of control the long term functionality of the structure will be improved because of preventing low cycle damage to the frame and bracing elements. The performance of SA-RBS is compared with the moment resisting frame (MRF), CBF and frame equipped with CC-RBS based on storey drift, damage indices and Fourier amplitude spectrum.

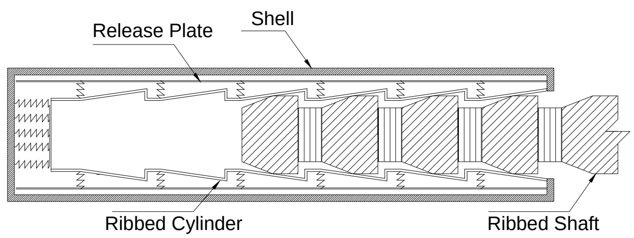

Figure 2. RBS (proposed by Golafshani et al.) [18].

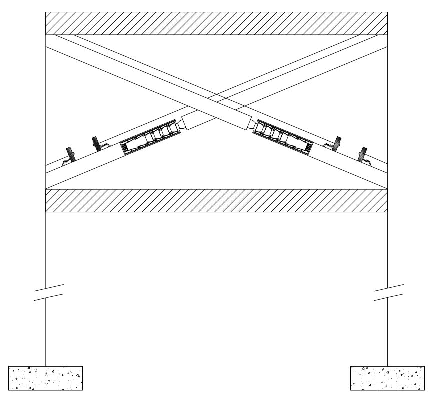

Figure 3. Structure equipped with RBS [18].

2. THE IDEA OF PRESENT WORK

The Semi-active device that proposed by Golafshani et al. is an improved model of the hook element with difference in its hysteresis loop. Conventional bracing systems ignoring of their compressive strength act similar to the hook element. These systems need large deformation to dissipate input energy from earthquake in hysteretic manner, because they move freely without enduring any force when enter in the compressive step (pinching or slipping). Also these systems cause to structures become stiffer and seismic energy needed to be absorbed by the structural system increased. RBS can endure only tension force continuously without buckling in compression. Unlike the conventional brace, RBS equipped bracing system absorbed a more portion of input energy without causing large storey drift. Figure 4 shows the ability of RBS system in decreasing the plastic deformation in the hysteresis cycle of the developed system in contrast with the conventional brace which does not have this ability. However CC-RBS decreases the story drifts significantly but absorbed energy increase because the brace are active over the excitation duration. Thus by using of control criteria based on storey drift and by installing sensor in stories, under severe earthquake when stories drift exceeds from certain value assigned based on the operation, RBS will become active. Besides of decreasing the storey drift, SA-RBS leads to minimize the number of active braces during earthquake and therefore damage index in stories become more uniform and structural life increases because of decreasing in low cycle fatigue. Also by using of this strategy with change of stiffness over the height of structure, principle mode period of structure shifts to a larger value and modal participation factor of higher mode increase therefore base shear and seismic input energy decreased.

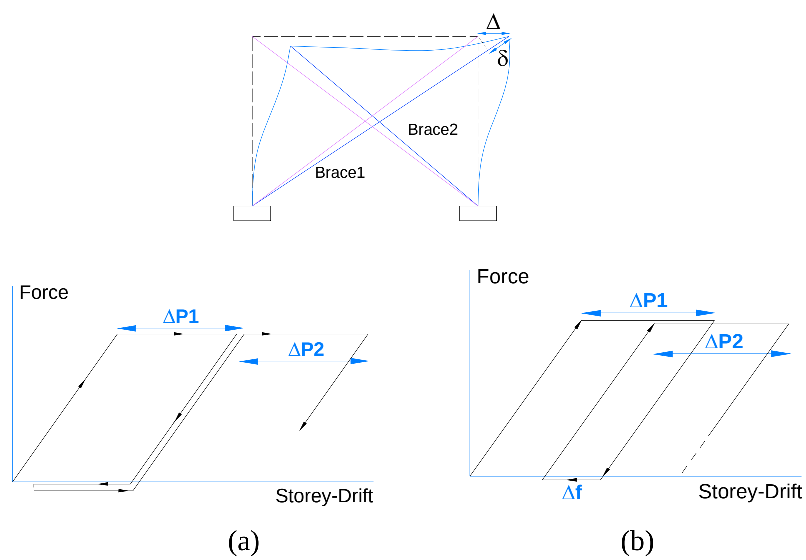

Figure 4. A single brace force-storey drift hysteresis loop: (a) Conventional brace; (b) RBS [18]

3. LENGTH-CORRECTION CONTROL SYSTEM

There is a problem in RBS equipped brace that if in the excitation time history the brace enters the compressive step and because of locking the ribs of shaft and cylinder in RBS, the shortened length is more than the deformation of the brace, so the brace could not return to its usual condition and the brace will be shorter than its original length and it causes a permanent deformation at the end of the excitations. Therefore a device should control the brace to endure tensile force in a determined tolerance in the compressive displacement region or set this tolerance to zero so the brace could not endure tensile force in the compressive displacement region. In other words the importance of the Length-correction system is preventing the permanent deflections at the end of the excitations. [18]

The mechanical system depicted in Figure 5, is the combination of a cable extended along the brace and two steel keys. Initially these two keys are adjusted apart by amount of tolerance, determined by designer and the cable is pre-tensioned. When the brace is shortened more than tolerance, two steel keys contact each other and the electronic switch releases the ribbed shaft by moving the release plate depicted in Figure 2 toward the shell. By adjusting the tolerance to zero, the brace does not endure any force in the compressive displacement region. On the contrary, by lengthening the brace two steel keys are disconnected and the ribbed shaft will be locked, so by interaction of shaft ribs and cylinder the brace endures tensile force.

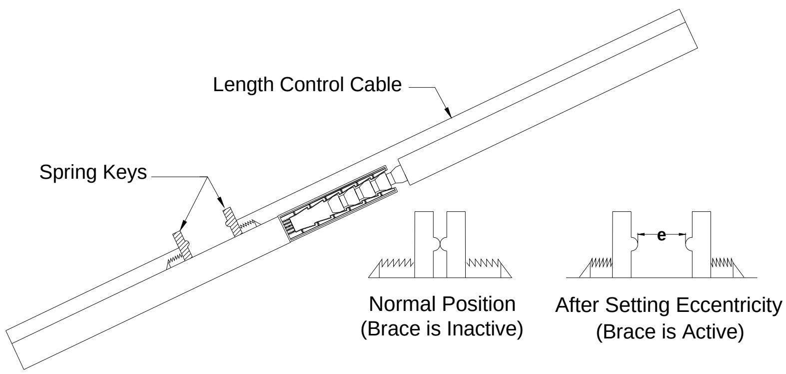

Figure 5. Length-correction control system [18].

4. MODIFIED PARK-ANG DAMAGE INDEX

In order to assess the behaviour of structure in severe earthquakes it has been used a damage index model. The damage model used in this research is the modified Park-Ang model in equation (1) that its difference with the original model (Park and Ang [19]) is subtracting the monotonic energy from the hysteretic energy of the member (Chai et al. [20]).

$$DI^*{}_{PA} = \frac{\Delta_m}{\Delta_{um}} + \frac{\beta^*(E_h - E_{hm})}{V_y \Delta_{um}} \tag{1}$$

$$\frac{\beta^*}{\beta} = \frac{\mu_m}{\mu_m + (1-\mu_m)\beta} \tag{2}$$

In which:

Δ_m =Maximum plastic deformation of member in the time history

Δ_{um} =Ultimate deformation of member in monotonic load

β , β^* =Conventional and modified Park-Ang factors respectively

E_h =Hysteresis energy of member

E_{hm} =The monotonic energy of member

V_y =Yield strength of member

In the simple elasto-plastic case, the monotonic energy is:

$$E_{hm} = V_y(\Delta_{um} - \Delta_y) \tag{3}$$

Where Δ_y is the yield deformation of member.

In RBS equipped braces since the brace moves freely in compression, the brace drift is not equal to brace plastic deformation used in damage index, therefore the cumulative plastic deformation should be calculated, so the free motion vector in each cycle should be subtracted from the total brace drift, Figure 6. Therefore the maximum deformation Δ_m in the damage index is:

$$\Delta_m = U_{last} - \sum_{i=1}^{n} \Delta f_i \tag{4}$$

Where:

n =number of cycles

U_{last} =Deflection at the time of calculating damage index

$\Delta f_i = \Delta_{i+1} - \Delta_i$ =i-th free motion vector in each cycle

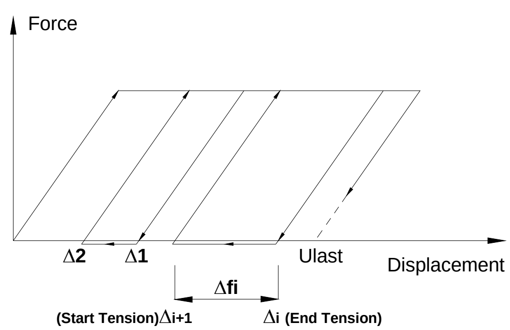

Figure 6. Calculating maximum deformation [18]

5. ANALYTICAL DESCRIPTION OF BILINEAR SYSTEMS HYSTERETIC LOOP

Mostaghel presented physically based analytical models capable of describing the behaviour of general hysteretic systems.[21] In the following bilinear hysteretic model without the effect of strength or stiffness loss that is suitable for steel structure is described and used for the modeling of frame hysteresis behaviour.

Consider a single-degree-of-freedom system composed of a mass *m*, two springs, viscous damper with a damping constant *c*. The spring of stiffness αk is directly connected to the mass. The deformation of this spring is represented by *x*. The other spring has stiffness $(1-\alpha)k$ and is connected to the mass by means of a slider with friction coefficient μ. The deformation of this spring is represented by *u*. *k* denotes the total stiffness of the two springs, and $\alpha \leq 1$ is the stiffness ratio. The applied force is defined by $P(t) = \overline{P}_0\, p(t)$, where $\overline{P}_0$ is its amplitude and *p*(*t*) is a nondimensional function of time. The force displacement relation, as portrayed in Figure 7, not including the viscous-damping force, can be expressed by

$$F = \alpha kx + (1-\alpha)ku \tag{5}$$

Where *u* = deformation of the spring connected to the slider. The slope of each segment, OA, BC, and DE, represents the total stiffness of the springs and is equal to *k*. The maximum force in the slider, the Coulomb friction force, is given by

$$\mu gm = (1-\alpha)k\delta \tag{6}$$

Where δ represents the spring's limiting deformation (the system's yield displacement) as defined by (6). Therefore, $-\delta \leq u \leq \delta$. Also

$$x_S(t) = x(t) - u(t) \tag{7}$$

Where $x_s(t)$ = sliding displacement of the slider. It is clear that the case $\alpha = 1$ represents linear systems, and the $\alpha = 0$ represents elastic perfectly plastic systems. Considering (5) and including viscous damping, the equation governing the motion of the system is

$$m\ddot{x} + c\dot{x} + \alpha kx + (1-\alpha)ku = \overline{P}_0\, p(t) \tag{8}$$

This equation involves two unknowns, *x* and *u*. A second equation can be obtained by characterizing the behaviour of the system. The following statements characterize the system's ideal bilinear behaviour, portrayed in Figure 7:

- The velocity, $\dot{x} = \partial x/\partial t$, along paths OA, DE, and EAB is positive and along paths BC and CD is negative.
- Because *u* is the deformation of the spring connected to the slider, as long as the system is in a sliding mode, the deformation in this spring will remain constant. Therefore, along the sliding paths EAB and CD, the velocity $\dot{u} = 0$, and along the nonsliding paths OA, BC, and DE, the velocity $\dot{u} = \dot{x}$.
- Further, along the path BC the spring deformation $u \geq -\delta$, while along the path DE $u \leq \delta$.

The simultaneous solution of (8) and above preceding statement defines the response of any nondegenerating hysteretic bilinear system under a given load. This model extended and used to describe the behaviour of bilinear multi-degree-of freedom systems. (Mostaghel and

Byrd [22])

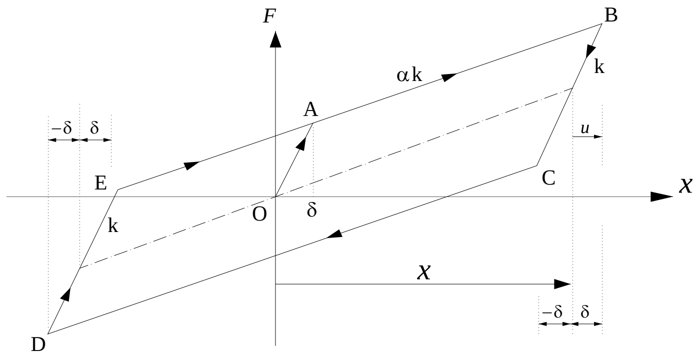

Figure 7. Hysteretic Loop for Bilinear System [21]

6. NONLINEAR DYNAMIC ANALYSIS

For the RBS equipped structure the horizontal vibration of an n-storey structure is modeled by the first n modes of the natural vibration of system. There are n principal degrees of freedom (DOF) for the floors. The finite element model of this dynamic system is shown in Figure 8a.

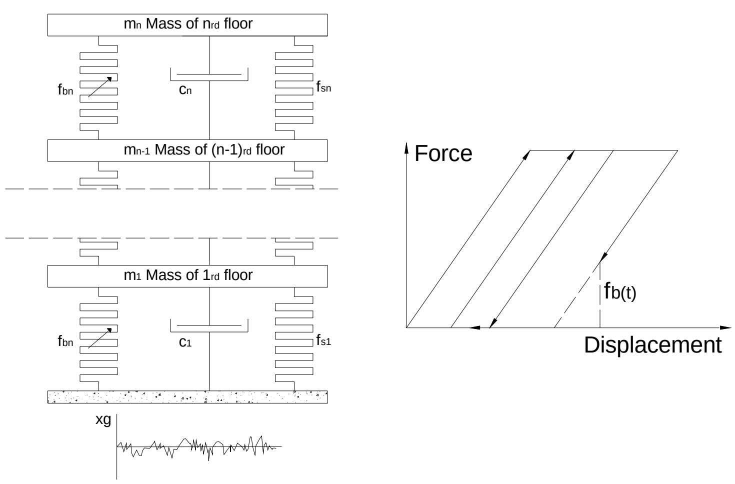

(a) (b)

Figure 8. (a) Finite element model; (b) brace resisting force

A nonlinear analysis computer code is prepared by Monzavi [23], which is capable of modeling the conventional braces with the hook element and considering the simple elasto-plastic behaviour for braces and bilinear elasto-plastic for moment frames by using of the above analytical model with $\alpha = 0.05$, also the computer code is capable of modeling the braces equipped with SA-RBS and CC-RBS

The second-order matrix equation of the reduced model by static condensation method may be written as follow:

$$M\ddot{x}(t) + C\dot{x}(t) + F_b(t) + F_s(t) = -Mr_g\ddot{x}_g(t) \tag{9}$$

Where M and C are the mass and proportional Rayleigh damping (ξ=0.05) matrices respectively, and F_s is the moment frame resisting force vector. F_b is the resisting force vector variable according to situation of the ribbed braces during the excitation, Fig 8.b. r_g is a location vector shows the extent and distribution of excitations on each DOF.

7. CASE STUDIES

In order to investigate the performance of CC-RBS and SA-RBS system in retrofitting the exist MRF, in contrast with CBS, a 10-storey MRF is considered shown in Figure 9. Because of investigating the effect of different retrofitting systems include CBS, CC-RBS and SA-RBS, moment resisting frame designed for 20 percent of code shear base is considered. The analyses have been carried out for MRF, MRF+CBF and both MRF+(CC-RBS) and MRF+(SA-RBS). Control limit used in this study is based on the maximum allowable storey drift presented in design building code. Maximum inelastic storey drift based on IBC code is as follow:

$$\overline{\Delta}_m < 0.025h \quad T < 0.7 \tag{10}$$

$$\overline{\Delta}_m \leq 0.02h \quad T \geq 0.7 \tag{11}$$

In order to investigate different retrofitted systems for existing moment resisting frame, Elcentro (1940) record is used and scaled for design base earthquake. Scaled PGA for design base earthquake (DBE) for Elcentro is 0.47g. (Figure 10)

The outputs are as follows:

- Maximum drift of stories
- Damage index of stories and global damage index
- Roof displacement time history
- Fourier amplitude spectra of stories response

The eigenfrequencies of moment frame and braced frame are obtained from eigenvalue analysis. Moment frame and braced frame principle frequency of two first modes are 0.42, 1.08 Hz and 0.84, 2.18 respectively.

In order to compare the result of various strategies the energy balance diagram and hysteresis loop of CBS and both SA-RBS and CC-RBS are depicted in Figures 11 and 12. It is shown in Figure 11 the excitation input energy [24] distributed in the forms of hysteresis energy, damping energy and kinetic energy in MRF, CBF, CC-RBS and SA-RBS based on

80 percent of maximum allowable storey drift. CC-RBS increases the stiffness of the structure, therefore input seismic energy is increased; also because of its hysteresis loop behaviour, it absorbs more portion of input energy in hysteretic form. In structures equipped with SA-RBS the amount of input energy is decreased and the total hysteretic energy of structure decreased too because of reduction in storey drifts.

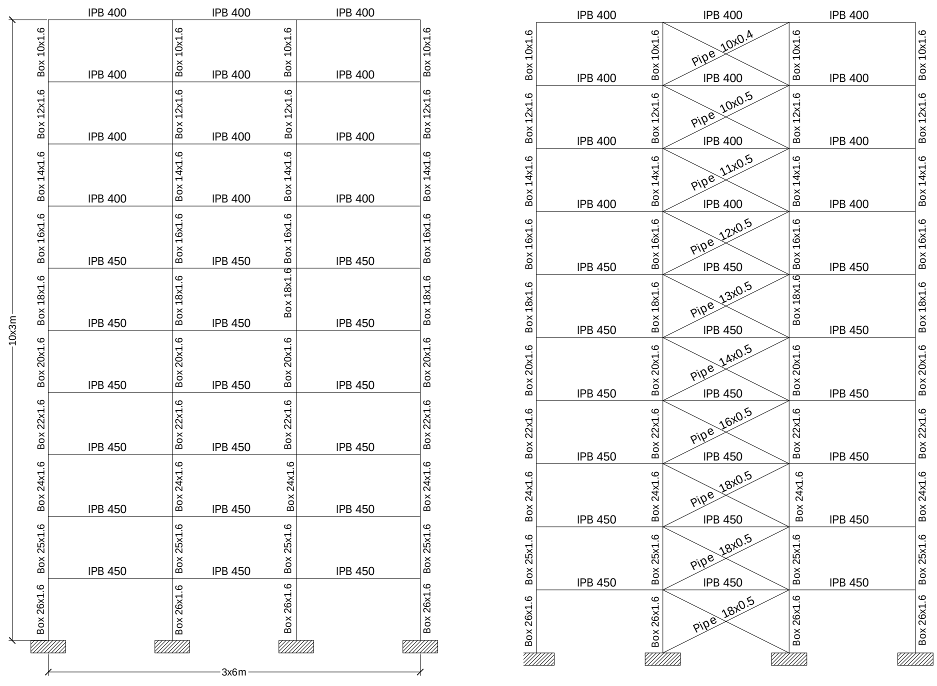

(a) (b)

Figure 9. Frame-elevation of case study structures: (a) moment resisting frame; (b). braced frame

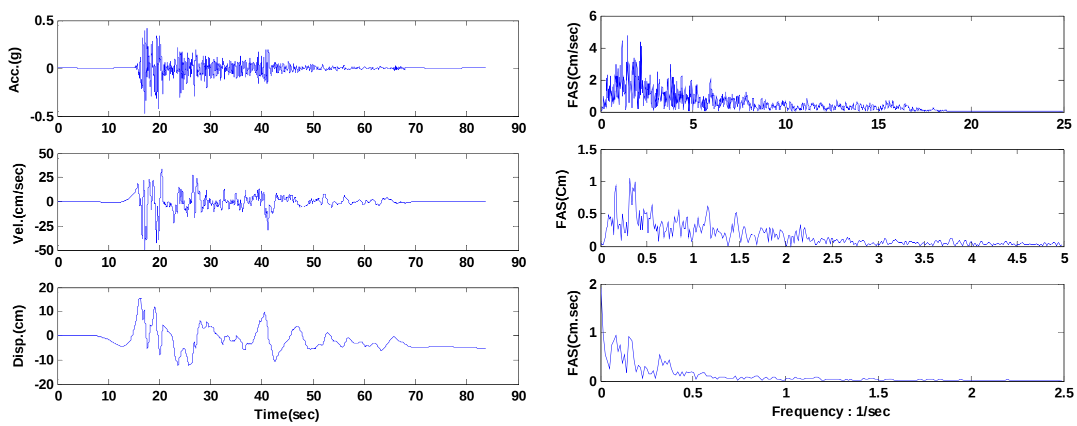

(a) (b)

Figure 10. Elcentro (1940), PGA=0.47g: (a) time history; (b) Fourier amplitude spectrum

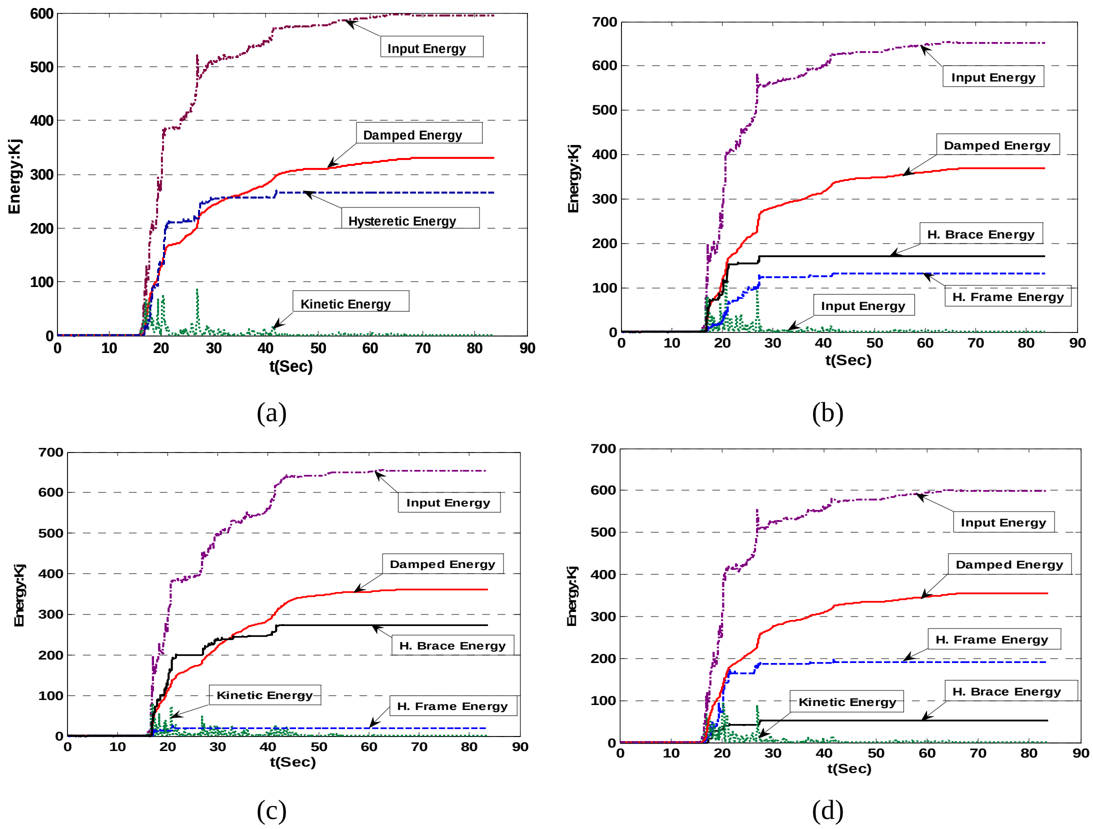

Figure 11. 10-storey structure energy distribution: (a) MRF, (b) CBS, (c) CC-RBS and (d) SA-RBS 80% All. Drift

Figure 12 shows the hysteresis loop of the CBS, CC-RBS and SA-RBS and hysteresis loop of the moment frame. In contrast with the CBS, hysteresis energy of the moment frame in SA-RBS is decreased and CC-RBS cause the storey remains elastic because of its ability to endure tension force continuously.

Fourier amplitude spectrum (FAS) of roof response obtained from finite Fast Fourier Transform (FFT) algorithm. The frequency content of roof total acceleration is depicted in Figure 13a. In contrast with CBS and CC-RBS, SA-RBS cause to shifting the principle mode period to a higher value and decreasing the total acceleration because more flexibility rather than other proposed systems.

Also in Figure 13b it is shown FAS of roof displacement. This shifting period is evident and CC-RBS cause to decreasing the roof displacement of MRF.

Comparing Figure 10 and Figure 13 it is seen that the peaks of displacements of systems is related to the Fourier amplitudes of velocity of input motion because of long period of the structure. Other peaks in Figure 13 are related to the structural natural frequencies.

Frequency domain response of the 6th storey for various retrofit systems is illustrated in Figure 14. This Figure show that SA-RBS cause to shift the frequency of braced frame to a lower value and decrease the response of MRF. Fourier amplitude spectrum of the first storey response of MRF and equipped frame are depicted in Figure 15. This Figure shows that frequency content of SA-RBS is similar to the MRF with smaller value.

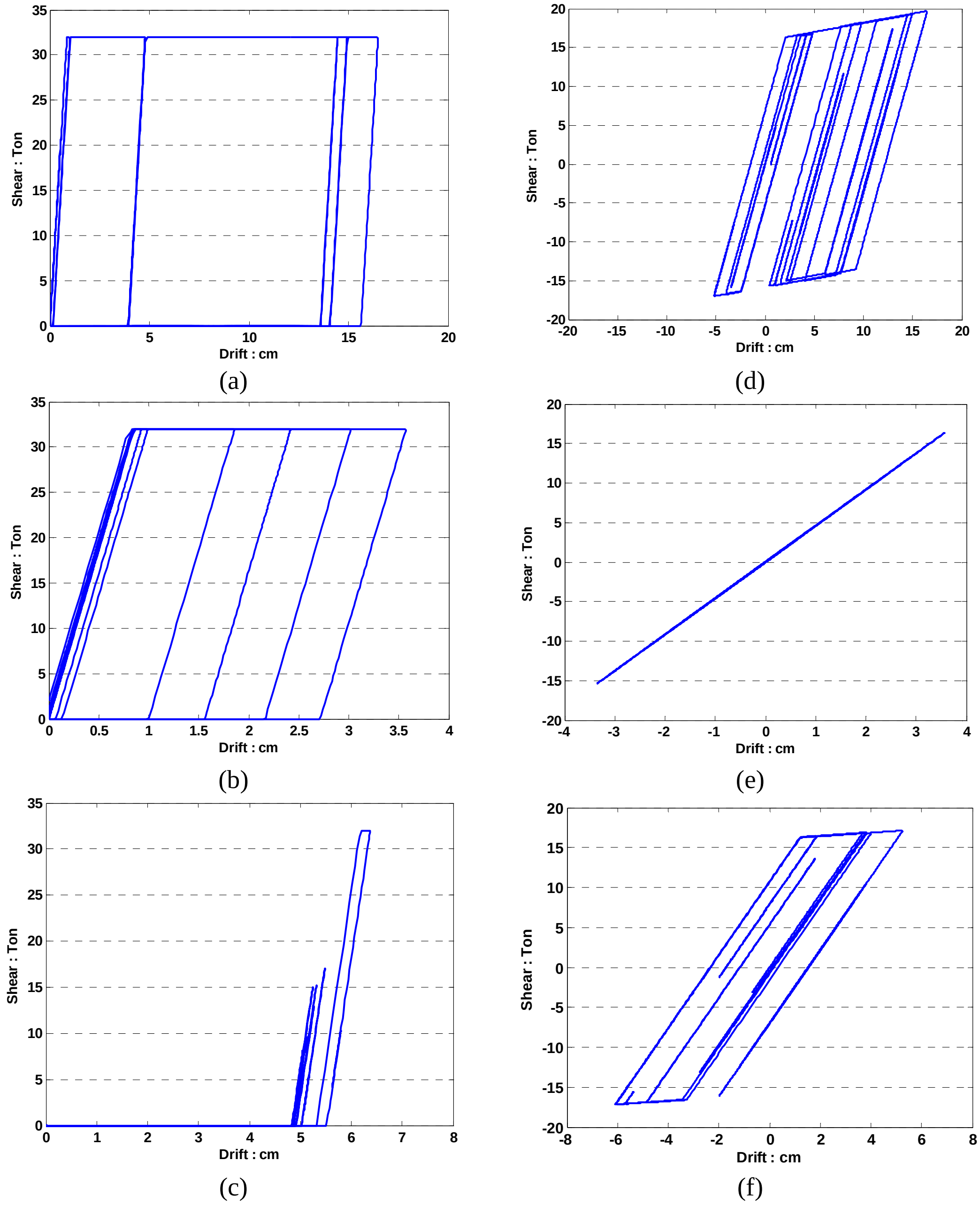

Figure 12. Storey-9 hysteresis loops: (a) CBS; (b) CC-RBS; (c) SA-RBS 80% All. Drift; (d) moment frame of CBS; (e) moment frame of CC-RBS; (e) moment frame of SA-RBS 80% Allowable. Drift

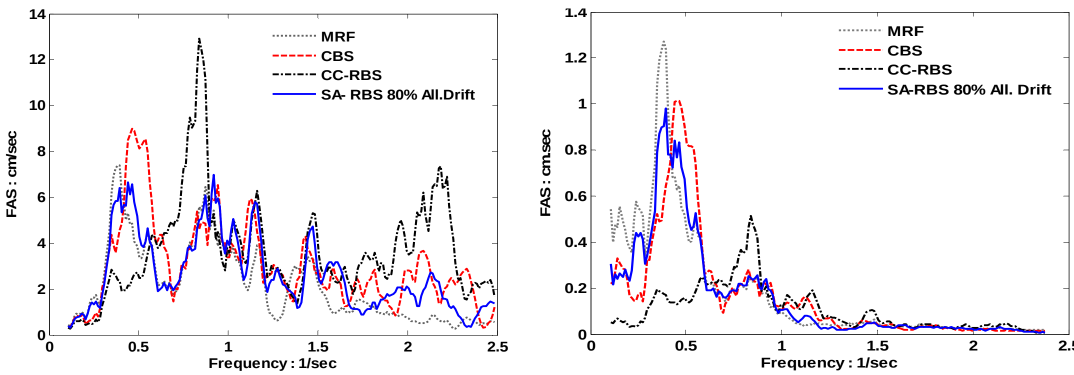

(a) (b)

Figure 13. Frequency content of roof response: (a) total acceleration; (b) storey displacement

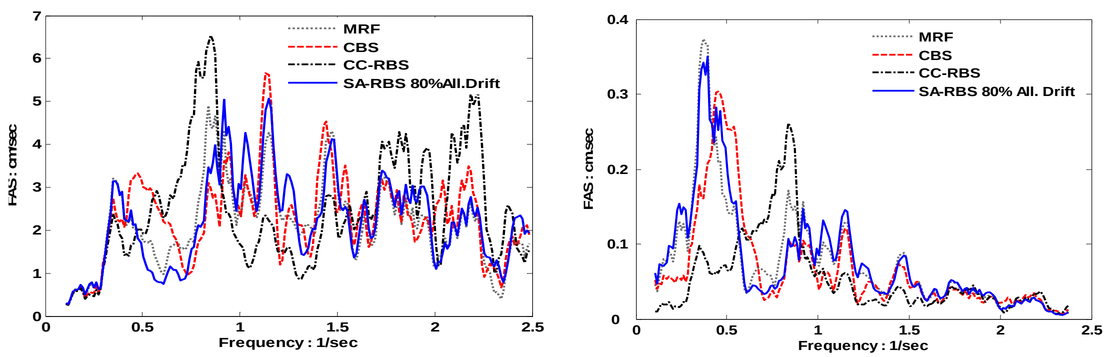

(a) (b)

Figure 14. 6th storey frequency domain response: (a) total acceleration; (b) storey displacement

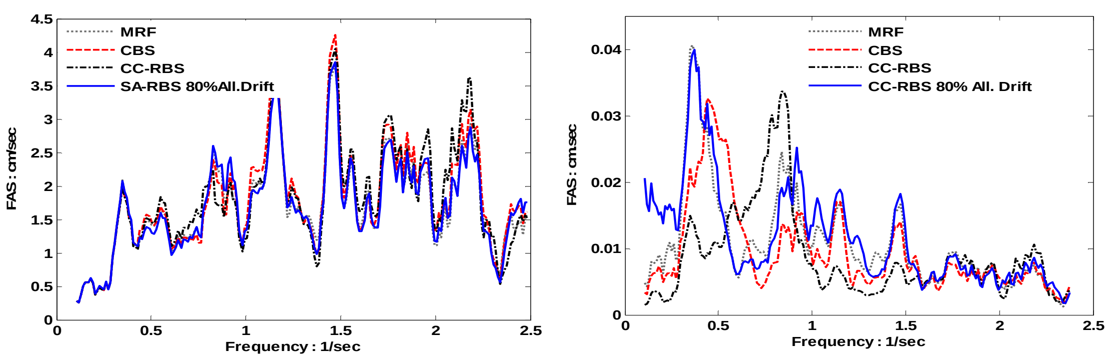

(a) (b)

Figure 15. 1th storey frequency domain response: (a) total acceleration; (b) storey displacement

From the analysis of 10-storey structure under Elcentro record, the roof displacement (Figure 16a-c) shows considerable decreasing approximately 60% in the peak displacement for structure equipped with CC-RBS and 30% for two other retrofit systems against of MRF.

It is seen in Figure 17.a that the maximum storey drifts are decreased in the 7, 8, 9 and 10-th stories in the SA-RBS base on 60 and 80 percent of allowable storey drift in contrast with MRF. However these values are more than CC-RBS and CBS but they are below the allowable drift limit and cause distribution of upper storey drift and total structure became more uniform. Figure 17.b shows that SA-RBS caused upper storey damage indices decrease. In Figure 17.c it is seen that in the SA-RBS with minimum number of tension bracing system during of earthquake excitation, global damage index decrease, and it is slightly more than that of CC-RBS.

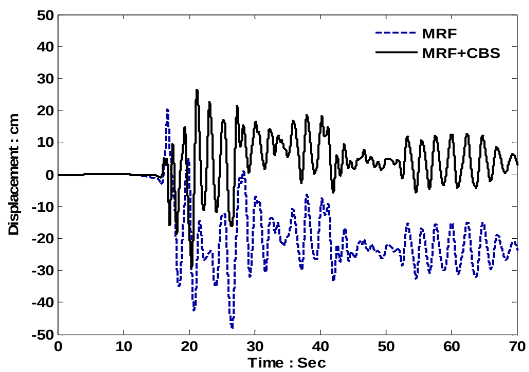

(a)

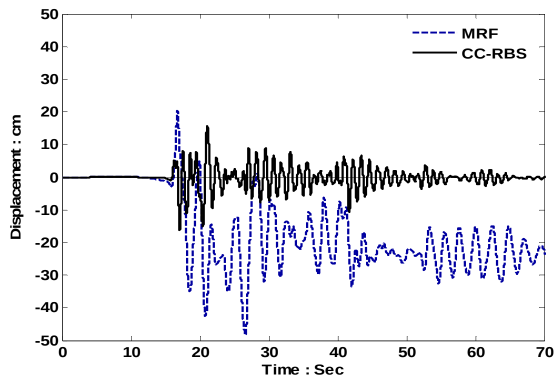

(b)

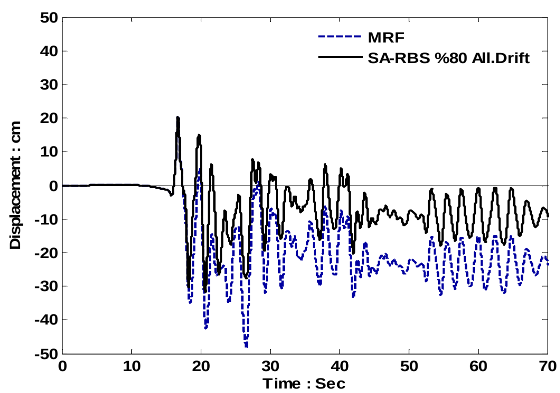

(c)

Figure 16. Roof displacement time history, (a) MRF+CBS, (b) MRF+(CC-RBS), (c) MRF+(SA-RBS) %80 Allowable. Drift

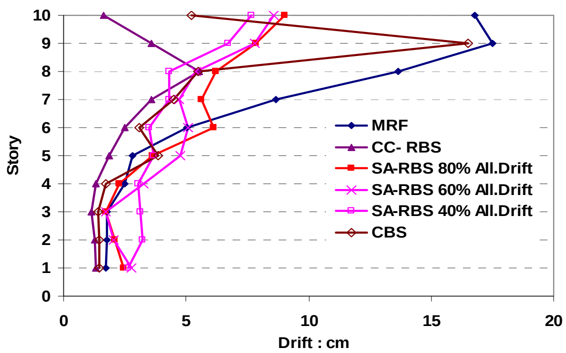

(a)

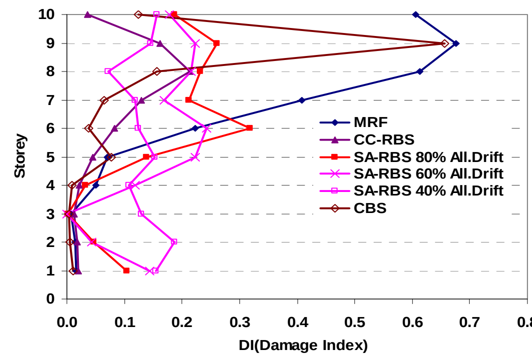

(b)

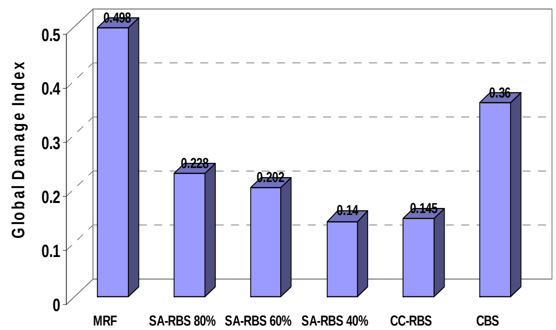

(c)

Figure 17. (a) Maximum storey drifts; (b) Storey damage index (DI); (c) Global damage index.

Figure 18a-c shows the time history of base shear in various retrofit systems. It is obvious that CC-RBS equipped frame has most base shear because of continuous stiffness presence during earthquake. But base shear of moment frame equipped with SA-RBS is smaller than other two systems; this structure has larger principle period of excitation, therefore earthquake force is decreased.

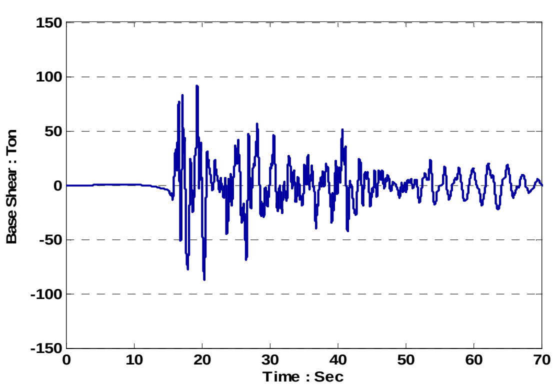

(a)

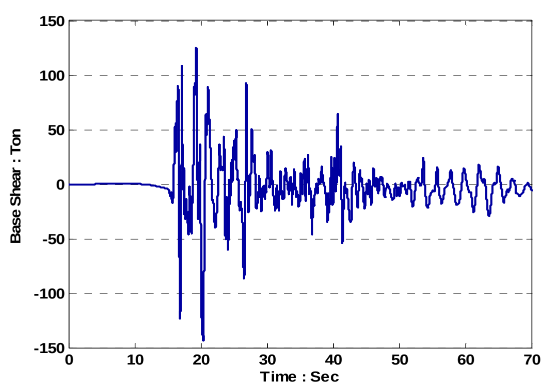

(b)

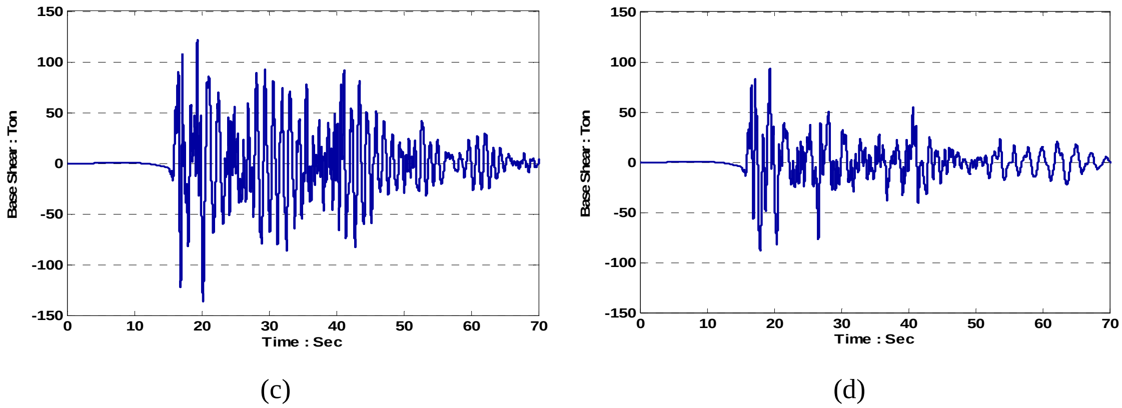

Figure 18. Base shear force: (a) MRF, (b) MRF+CBS, (c) MRF+(CC-RBS), (d) MRF+(SA-RBS) %80 Allowable. Drift

Figure 19 shows distribution of storey shear in height of structure that retrofitted with various systems. Shear force in stories 1-5 in structure equipped with SA-RBS system is equal to the MRF because RBS in this storey remain off during Elcentro earthquake.

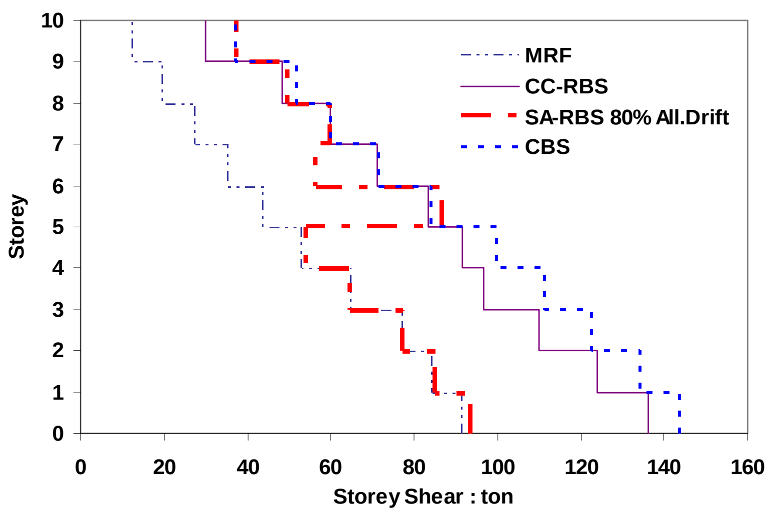

Figure 19. Maximum storey shear

8. CONCLUSIONS

With installing sensors in stories and obtaining storey drifts in short time steps, proposed RBS could be controlled based on a simple algorithm. In this paper performance of various systems including of conventional brace system (CBS), completely closed RBS (CC-RBS) and semi-active RBS (SA-RBS), in retrofitting of an existing moment resisting frame (MRF) has been investigated. However CC-RBS leads to minimum response among proposed systems, but using of SA-RBS cause to minimum number of RBS to be active during earthquake excitation and structural response became below the maximum allowable storey drift. The ability of variable stiffness leads to period shifting and therefore base shear is decreased. Reduction in base shear is very important from structural performance point of view. The more reduction in the base shear, the more low-cycle fatigue life of the structure. SA-RBS cause shifting in principle period of the structure to a larger value, therefore input energy of excitation and base shear decrease.

REFERENCES

1. Soong TT, Spencer BF. Supplemental energy dissipation: state-of-the-art and state-of-the-practice, *Engineering Structures*, **24**(2002) 243–59.
2. Spencer BF, Nagarajaiah S. State of the Art of Structural Control, *Journal of Structural Engineering ASCE*, **129**(2003)845-56.
3. Symans MD, Constantinou MC. Semi-active control systems for seismic protection of structures: state-of-the-art review, *Journal of Structural Engineering ASCE*, **125**(1999) 469–87.
4. Spencer BF, Dyke SJ, Deoskar HS. Benchmark problem in structural control, Part I: active mass driver system, *Proceedings of the ASCE Structures Congress*, Portland. 1997.
5. Spencer BF, Dyke SJ, Deoskar HS. Benchmark problem in structural control, Part II: active tendon system, *Proceedings of the ASCE Structures Congress*, Portland. 1997.
6. Higashino M, Aizawa S. Application of active mass damper system in actual buildings. In: Housner GW, Marsi SF, editors, *Proceedings of the International Workshop on Structural Control*, Los Angeles, CA. 1993, pp. 194-205.
7. Soong TT, Reinhorn AM, Aizawa S, Higashino M. Recent structural applications of active control technology, *Journal of Structural Control*, **1**(1994) 5–21.
8. Chunxiang L, Yanxia L. Active multiple tuned mass dampers for structure under the ground acceleration, *Earthquake Engineering ans Suractural Dynamics* **31**(2002) 1041–52.
9. Gavin HP, Hanson RD, Filisco FE. Electrorheological dampers, Part I: analysis and design, *Journal of Applied Mechanics*, **63**(1996) 669–75.
10. Spencer BF, Dyke SJ, Sain MK, Clarson JD. Phenomenological model for magnerheological dampers, *Journal of Engineering Mechanics ASCE*, **123**(1997) 30–8.
11. Fujita T, Shimazaki M, Yutaka H, Aizawa S, Higashino M, Haniuda N. Semi-active seismic isolation system using controllable friction damper, *Bulletin of Earthquake Resistant Structure Research Center*, **27**(1994) 21–31.
12. Symans MD, Constantinou MC. Seismic testing of a building structure with a semi active fluid damper control system, *Earthquake Engineering and Structural Dynamics*, **26**(1997) 759–77.
13. Nemer DC, Lin Y, Osegueda RA. Semi-active motion control using variable stiffness, *Journal of Structural Engineering*, **22**(1994) 925–41.

14. Yang JN, Wu JC, Li Z. Control of seismic excited buildings using active variable stiffness, *Engineering Structures*, **18**(1996) 589–96.
15. Nagarajaiah S. Semi active control of structures, *Proceedings of the Structures Congress XV*, ASCE, Potland, OR. 1997, pp. 1574–1578.
16. Kobori T, Takahashi M, Nasu T, Niwa N, Ogasawara K. Seismic response controlled structure with active variable stiffness system, *Earthquake Engineering and Structural Dynamics*, **22**(1993) 925–41.
17. Golafshani AA, Mirdamadi HR. Adaptive control of structures by LMS Algorithm: a comparative study, *Structures & Buildings*, **152**(2001) 175–91.
18. Golafshani AA, Kabiri Rahani E, Tabeshpour MR. A new high performance semi-active bracing system, *Engineering Structures*, **28**(2006) 1972–82.
19. Park YJ, Ang HS, Eeri M, Wen YK. Damage-limiting a seismic design of buildings, *Earthquake Spectra*, **3**(1987) 1–26.
20. Chai YH, Romstad KM, Bird SM. Energy-based linear damage model For high-intensity seismic loading, *Journal of Structural Engineering ASCE*, **121**(1995) 857–64.
21. Mostaghel N. Analytical description of pinching, degrading hysteretic system, *Journal of Engineering Mechanics ASCE*, **125**(1999) 216–24.
22. Mostaghel N, Byrd RA. Analytical description of multi-degree bilinear hysteretic system, *Journal of Engineering Mechanics ASCE*, **126**(1999) 588–98.
23. Monzavi M. Seismic performance evaluation of steel frame with a new high performance semi-active bracing system, *M.Sc. thesis*. Sharif University of Technology, 2006.
24. Uang CM, Bertero VV. Evaluation of seismic energy in structures, *Earthquake Engineering and Structural Dynamics*, **19**(1990) 77–90.